Inverse Scattering Bayesian Compressive Sensing Techniques under the Rytov Approximation - Presentation and Preliminary Assessment

L. Poli, G. Oliveri, P. Rocca, A. Massa

Abstract

In this report, the basic formulation of an inverse scattering problem under the Rytov approximation is presented. The single-task Bayesian compressive Sensing technique is then applied to invert the scattered data. Finally, the calibration procedure of the BCS parameters together with some preliminary results dealing with small objects are reported.

Contents

1 Mathematical Formulation

1.1 The Rytov Approximation

It is possible to derive the Rytov approximation [?] by considering the total field represented as

$$E_{tot}(\overrightarrow{r}) = e^{\phi(\overrightarrow{r})} \tag{1}$$

where ϕ is the total phase defined as the sum of the incident phase function ϕ_0 and the scattered complex phase ϕ_s:

$$\phi(\overrightarrow{r}) = \phi_0(\overrightarrow{r}) + \phi_s(\overrightarrow{r}) \tag{2}$$

and

$$E_{inc}(\overrightarrow{r}) = e^{\phi_0(\overrightarrow{r})} \tag{3}$$

is the incident field.

Starting form the wave equation

$$(\bigtriangledown^2 + k_0^2)E(\overrightarrow{r}) = 0 \tag{4}$$

we can rewrite it as follows:

$$(\bigtriangledown\phi(\overrightarrow{r}))^2 + \bigtriangledown^2\phi(\overrightarrow{r}) + k_0^2 = -\tau(\overrightarrow{r}) \tag{5}$$

It is possible to demonstrate [?] that the solution of the differential equation can be expressed as an integral equation:

$$E_{inc}(\overrightarrow{r})\phi_s(\overrightarrow{r}) = \int_{V'} G(\overrightarrow{r} - \overrightarrow{r}')E_{inc}(\overrightarrow{r}')\left[(\bigtriangledown\phi_s(\overrightarrow{r}))^2 + \tau(\overrightarrow{r}')\right] dr' \tag{6}$$

where $G(\overrightarrow{r} - \overrightarrow{r}')$ is the Green's function and $\tau(\overrightarrow{r})$ is the object function.

Under the Rytov approximation, it is assumed that the term in the above equation can be approximated by

$$(\bigtriangledown\phi_s(\overrightarrow{r}))^2 + \tau(\overrightarrow{r}') =\cong \tau(\overrightarrow{r}') \tag{7}$$

Then, the first-order Rytov approximation to the scattered phase ϕ_s becomes

$$\phi_s(\overrightarrow{r}) = \frac{2}{E_{inc}(\overrightarrow{r})} \int_{V'} G(\overrightarrow{r} - \overrightarrow{r}')E_{inc}(\overrightarrow{r}')\tau(\overrightarrow{r}')dr' \tag{8}$$

1.2 Inverse CS Problem under Rytov approximation

Using Compressive Sampling techniques it is possible to solve linear problems such as: given $\overline{y} = \overline{A} \cdot \overline{x}$ find $\overline{x}$ such that $\overline{x} \in C^M$ and $\overline{x}$ is sparse. Considering Rytov approximation and equation (8), we can define

$$\overline{y} = \begin{bmatrix} \phi_s\left(x_1, y_1\right) \\ ... \\ \phi_s\left(x_M, y_M\right) \end{bmatrix} \tag{9}$$

with size $M \times 1$, $m = 1, ..., M$ and $v = 1, ..., V$, where M is the number of measurement points and V is the number of views;

$$\overline{A} = \begin{bmatrix} \frac{G_{2d}^{ext}(\rho_{11})E_{inc}(x_1', y_1')}{E_{inc}(x_1, y_1)} & ... & \frac{G_{2d}^{ext}(\rho_{1N})E_{inc}(x_N', y_N')}{E_{inc}(x_1, y_1)} \\ ... & ... & ... \\ \frac{G_{2d}^{ext}(\rho_{M1})E_{inc}(x_1', y_1')}{E_{inc}(x_M, y_M)} & ... & \frac{G_{2d}^{ext}(\rho_{MN})E_{inc}(x_N', y_N')}{E_{inc}(x_M, y_M)} \end{bmatrix} \tag{10}$$

with size $M \times N$, $n = 1, ..., N$ where N is the number of cells in the investigation domain, and $\rho_{mn} = \sqrt{\left[\left(x_m - x_n'\right)^2 + \left(y_m - y_n'\right)^2\right]}$.

Finally the unknown's vector:

$$\overline{x} = \begin{bmatrix} \tau\left(x_1', y_1'\right) \\ ... \\ \tau\left(x_N', y_N'\right) \end{bmatrix} \tag{11}$$

2 Preliminary Assessment

2.1 TEST CASE: Calibration - Square Cylinder $L = 0.16\lambda$

Goal: show the performances of BCS when dealing with a sparse scatterer

- Number of Views: V
- Number of Measurements: M
- Number of Cells for the Inversion: N
- Number of Cells for the Direct solver: D
- Side of the investigation domain: L

Test Case Description

Direct solver:

- Square domain divided in $\sqrt{D} \times \sqrt{D}$ cells
- Domain side: $L = 3\lambda$
- $D = 1296$ (discretization for the direct solver: $< \lambda/10$)

Investigation domain:

- Square domain divided in $\sqrt{N} \times \sqrt{N}$ cells
- $L = 3\lambda$
- $2ka = 2 \times \frac{2\pi}{\lambda} \times \frac{L\sqrt{2}}{2} = 6\pi\sqrt{2} = 26.65$
- $\#DOF = \frac{(2ka)^2}{2} = \frac{(2\times\frac{2\pi}{\lambda}\times\frac{L\sqrt{2}}{2})^2}{2} = 4\pi^2\left(\frac{L}{\lambda}\right)^2 = 4\pi^2 \times 9 \approx 355.3$
- N scelto in modo da essere vicino a $\#DOF$: $N = 324$ (18×18)

Measurement domain:

- Measurement points taken on a circle of radius $\rho = 3\lambda$
- Full-aspect measurements
- $M \approx 2ka \rightarrow M = 27$

Sources:

- Plane waves
- $V \approx 2ka \rightarrow V = 27$
- Amplitude: $A = 1$
- Frequency: 300 MHz $(\lambda = 1)$

Object:

- Square cylinder of side $\frac{\lambda}{6} = 0.1667$
- $\varepsilon_r = 2.0$

- $\sigma = 0$ [S/m]

BCS parameters:

- Initial estimate of the noise: $n_0 = \in \{1.0 \times 10^{-6}, 2.0 \times 10^{-6}, 5.0 \times 10^{-6}, 1.0 \times 10^{-5}, 2.0 \times 10^{-5}, 5.0 \times 10^{-5}, 1.0 \times 10^{-4}, 2.0 \times 10^{-4}, 5.0 \times 10^{-4}, 1.0 \times 10^{-3}, 2.0 \times 10^{-3}, 5.0 \times 10^{-3}, 1.0 \times 10^{-2}\}$
- Convergenze parameter: $\tau = 1.0 \times 10^{-8}$

RESULTS: Calibration

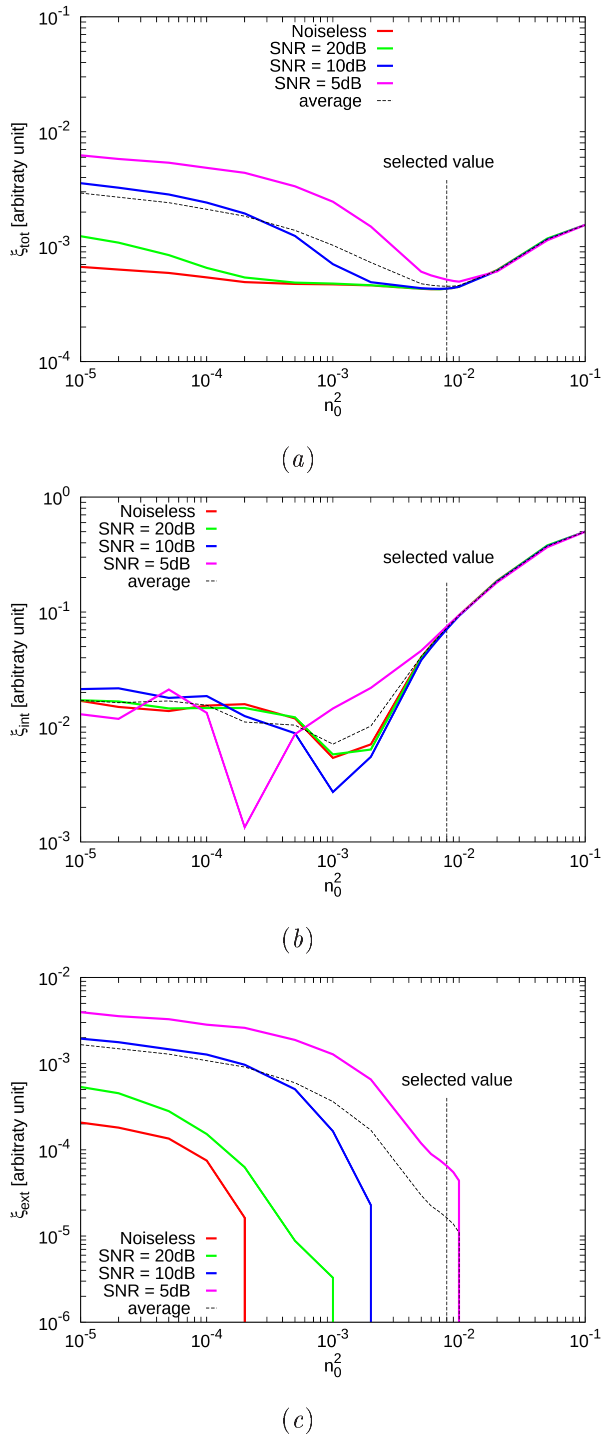

Figure 1. Behaviour of error figures as a function of the initial estimate of the noise n_0, for different SNR values: (a) total error ξ_{tot}, (b) internal error ξ_{int}, (c) external error ξ_{ext}.

2.2 TEST CASE: Square Cylinder $L = 0.16\lambda$

Goal: show the performances of BCS when dealing with a sparse scatterer

- Number of Views: V
- Number of Measurements: M
- Number of Cells for the Inversion: N
- Number of Cells for the Direct solver: D
- Side of the investigation domain: L

Test Case Description

Direct solver:

- Square domain divided in $\sqrt{D} \times \sqrt{D}$ cells
- Domain side: $L = 3\lambda$
- $D = 1296$ (discretization for the direct solver: $< \lambda/10$)

Investigation domain:

- Square domain divided in $\sqrt{N} \times \sqrt{N}$ cells
- $L = 3\lambda$
- $2ka = 2 \times \frac{2\pi}{\lambda} \times \frac{L\sqrt{2}}{2} = 6\pi\sqrt{2} = 26.65$
- $\#DOF = \frac{(2ka)^2}{2} = \frac{(2\times\frac{2\pi}{\lambda}\times\frac{L\sqrt{2}}{2})^2}{2} = 4\pi^2\left(\frac{L}{\lambda}\right)^2 = 4\pi^2 \times 9 \approx 355.3$
- N scelto in modo da essere vicino a $\#DOF$: $N = 324$ (18×18)

Measurement domain:

- Measurement points taken on a circle of radius $\rho = 3\lambda$
- Full-aspect measurements
- $M \approx 2ka \rightarrow M = 27$

Sources:

- Plane waves
- $V \approx 2ka \rightarrow V = 27$
- Amplitude: $A = 1$
- Frequency: 300 MHz ($\lambda = 1$)

Object:

- Square cylinder of side $\frac{\lambda}{6} = 0.1667$
- $\varepsilon_r \in \{1.5, 2.0, 2.5, 3.0\}$
- $\sigma = 0$ [S/m]

BCS parameters:

- Initial estimate of the noise: $n_0 = 8.0 \times 10^{-3}$
- Convergenze parameter: $\tau = 1.0 \times 10^{-8}$

RESULTS: Square Cylinder $L = 0.16\lambda$

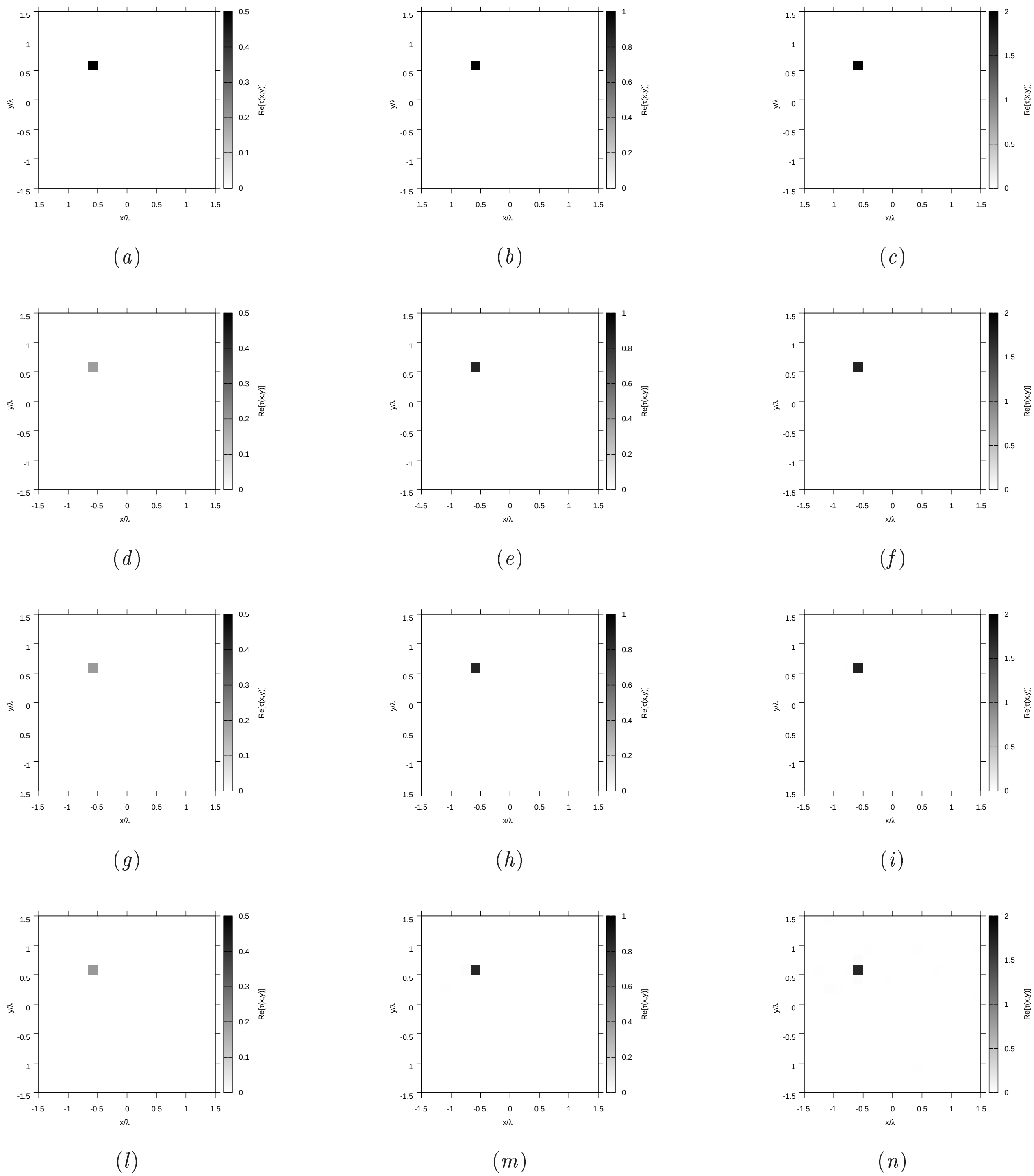

Figure 2. Actual object $(a)(b)(c)$ and BCS reconstructed object with $(d)(g)(l)$ $\varepsilon_r = 1.5$, $(e)(h)(m)$ $\varepsilon_r = 2.0$, and $(f)(i)(n)$ $\varepsilon_r = 3.0$, for $(d)(e)(f)$ Noiseless case, $(g)(h)(i)$ $SNR = 10$ [dB] and $(l)(m)(n)$ $SNR = 5$ [dB].

RESULTS: Square Cylinder $L = 0.16\lambda$ - Error Figures - Comparison Born/Rytov Approximation

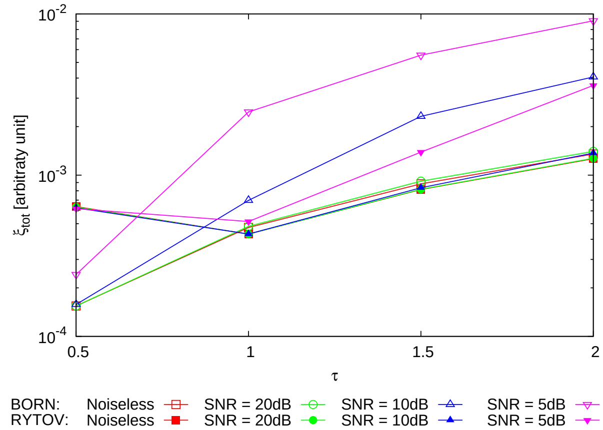

(a)

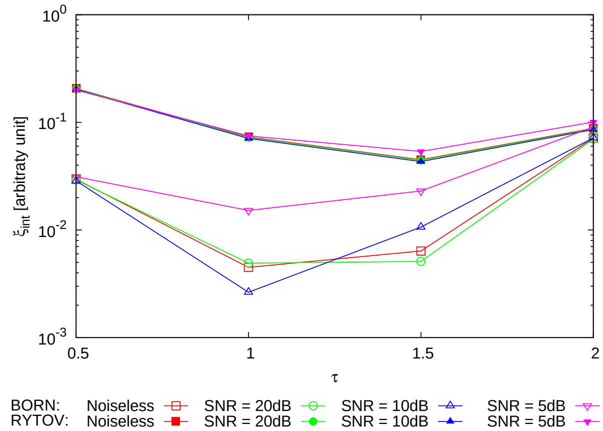

(b)

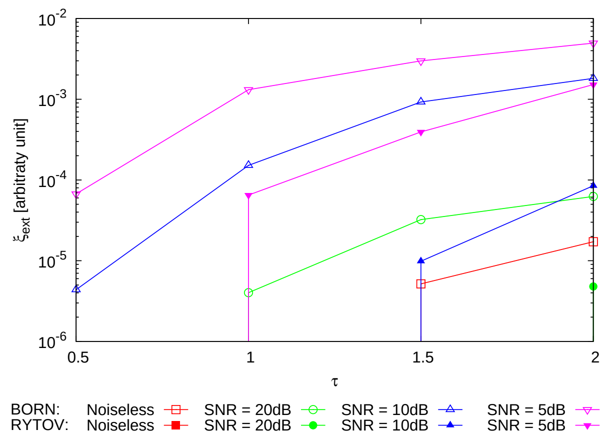

(c)

Figure 3. Behaviour of error figures as a function of ε_r, for different SNR values: (a) total error ξ_{tot}, (b) internal error ξ_{int}, (c) external error ξ_{ext}.

2.3 TEST CASE: Square Cylinder $L = 0.33\lambda$

Goal: show the performances of BCS when dealing with a sparse scatterer

- Number of Views: V
- Number of Measurements: M
- Number of Cells for the Inversion: N
- Number of Cells for the Direct solver: D
- Side of the investigation domain: L

Test Case Description

Direct solver:

- Square domain divided in $\sqrt{D} \times \sqrt{D}$ cells
- Domain side: $L = 3\lambda$
- $D = 1296$ (discretization for the direct solver: $< \lambda/10$)

Investigation domain:

- Square domain divided in $\sqrt{N} \times \sqrt{N}$ cells
- $L = 3\lambda$
- $2ka = 2 \times \frac{2\pi}{\lambda} \times \frac{L\sqrt{2}}{2} = 6\pi\sqrt{2} = 26.65$
- $\#DOF = \frac{(2ka)^2}{2} = \frac{(2\times\frac{2\pi}{\lambda}\times\frac{L\sqrt{2}}{2})^2}{2} = 4\pi^2\left(\frac{L}{\lambda}\right)^2 = 4\pi^2 \times 9 \approx 355.3$
- N scelto in modo da essere vicino a $\#DOF$: $N = 324$ (18×18)

Measurement domain:

- Measurement points taken on a circle of radius $\rho = 3\lambda$
- Full-aspect measurements
- $M \approx 2ka \rightarrow M = 27$

Sources:

- Plane waves
- $V \approx 2ka \rightarrow V = 27$
- Amplitude: $A = 1$
- Frequency: 300 MHz $(\lambda = 1)$

Object:

- Square cylinder of side $\frac{\lambda}{3} = 0.33$
- $\varepsilon_r \in \{1.5, 2.0, 2.5, 3.0\}$
- $\sigma = 0$ [S/m]

BCS parameters:

- Initial estimate of the noise: $n_0 = 8.0 \times 10^{-3}$
- Convergenze parameter: $\tau = 1.0 \times 10^{-8}$

RESULTS: Square Cylinder $L = 0.33\lambda$

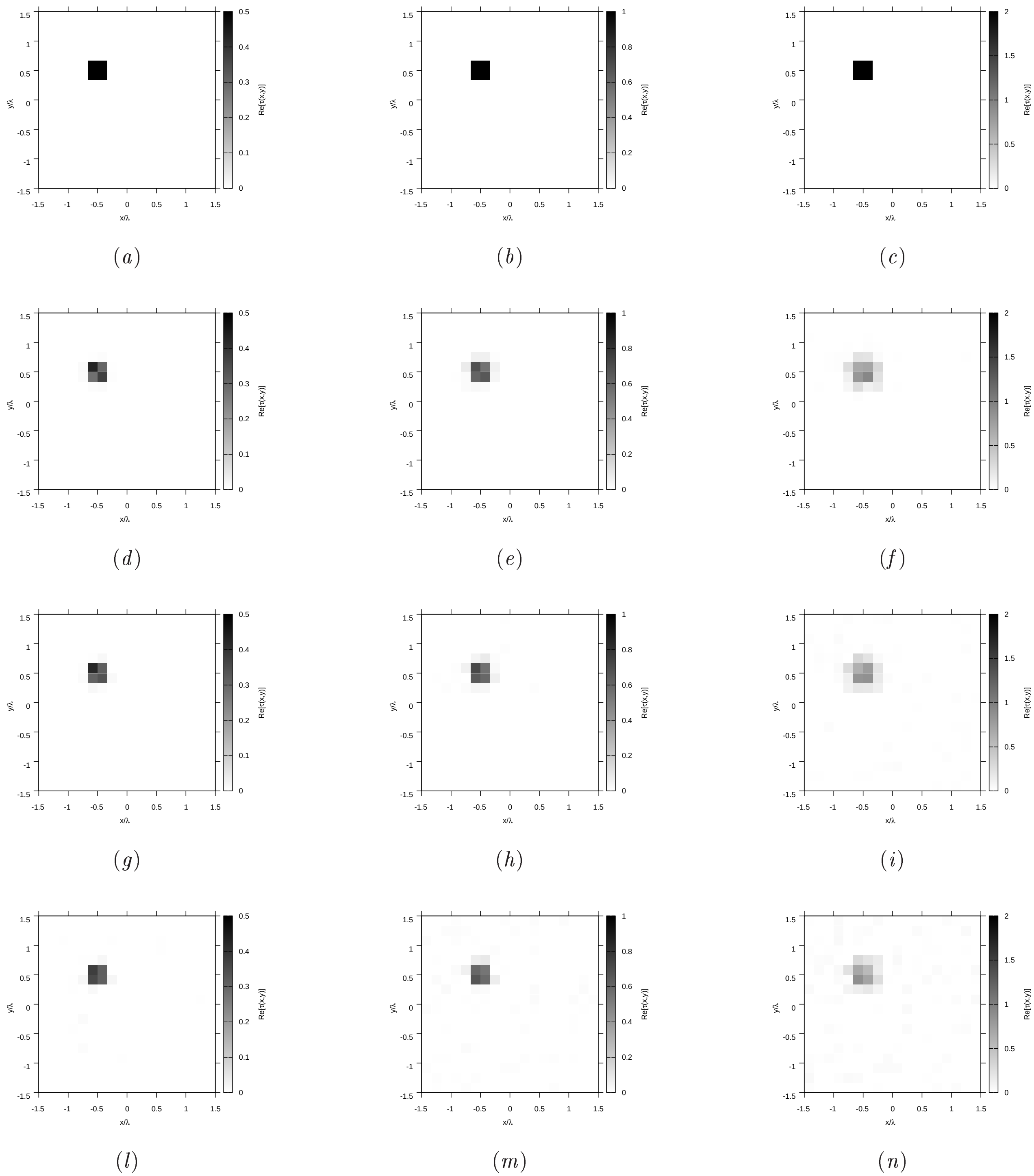

Figure 6. Actual object $(a)(b)(c)$ and BCS reconstructed object with $(d)(g)(l)$ $\varepsilon_r = 1.5$, $(e)(h)(m)$ $\varepsilon_r = 2.0$, and $(f)(i)(n)$ $\varepsilon_r = 3.0$, for $(d)(e)(f)$ Noiseless case, $(g)(h)(i)$ $SNR = 10$ [dB] and $(l)(m)(n)$ $SNR = 5$ [dB].

RESULTS: Square Cylinder $L = 0.33\lambda$ - Error Figures - Comparison Born/Rytov Approximation

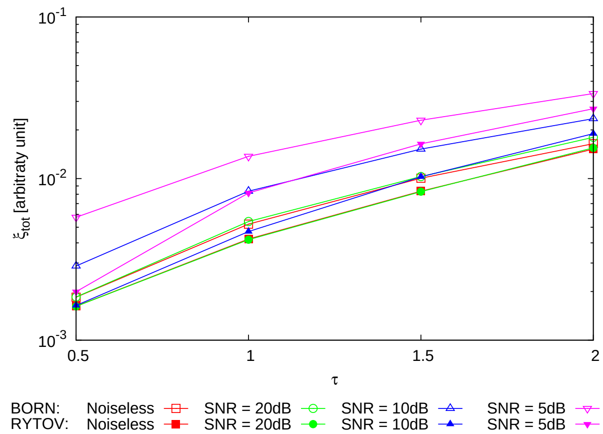

(a)

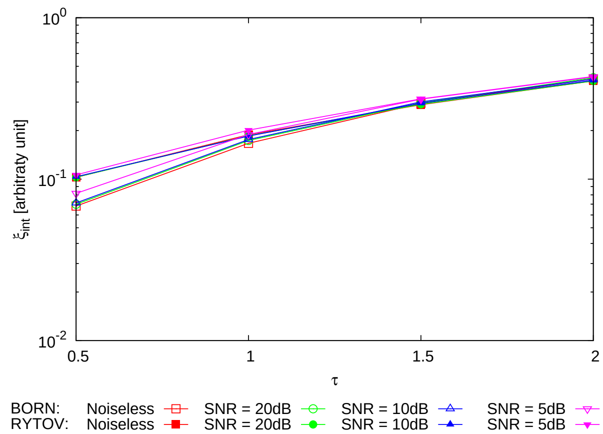

(b)

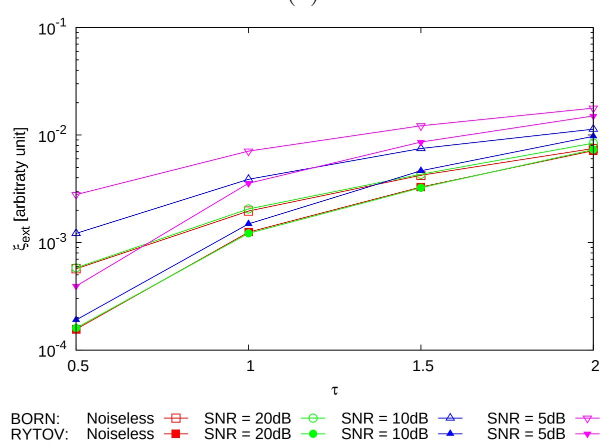

(c)

Figure 7. Behaviour of error figures as a function of ε_r, for different SNR values: (a) total error ξ_{tot}, (b) internal error ξ_{int}, (c) external error ξ_{ext}.

2.4 TEST CASE: Two Square Cylinders $L = 0.16\lambda$

Goal: show the performances of BCS when dealing with a sparse scatterer

- Number of Views: V
- Number of Measurements: M
- Number of Cells for the Inversion: N
- Number of Cells for the Direct solver: D
- Side of the investigation domain: L

Test Case Description

Direct solver:

- Square domain divided in $\sqrt{D} \times \sqrt{D}$ cells
- Domain side: $L = 3\lambda$
- $D = 1296$ (discretization for the direct solver: $< \lambda/10$)

Investigation domain:

- Square domain divided in $\sqrt{N} \times \sqrt{N}$ cells
- $L = 3\lambda$
- $2ka = 2 \times \frac{2\pi}{\lambda} \times \frac{L\sqrt{2}}{2} = 6\pi\sqrt{2} = 26.65$
- $\#DOF = \frac{(2ka)^2}{2} = \frac{(2\times\frac{2\pi}{\lambda}\times\frac{L\sqrt{2}}{2})^2}{2} = 4\pi^2\left(\frac{L}{\lambda}\right)^2 = 4\pi^2 \times 9 \approx 355.3$
- N scelto in modo da essere vicino a $\#DOF$: $N = 324$ (18×18)

Measurement domain:

- Measurement points taken on a circle of radius $\rho = 3\lambda$
- Full-aspect measurements
- $M \approx 2ka \rightarrow M = 27$

Sources:

- Plane waves
- $V \approx 2ka \rightarrow V = 27$
- Amplitude: $A = 1$
- Frequency: 300 MHz ($\lambda = 1$)

Object:

- Two square cylinders of side $\frac{\lambda}{6} = 0.1667$
- $\varepsilon_r \in \{1.5, 2.0, 2.5, 3.0\}$ (two square), $\varepsilon_r = 1.9$ (one square)
- $\sigma = 0$ [S/m]

BCS parameters:

- Initial estimate of the noise: $n_0 = 8.0 \times 10^{-3}$
- Convergenze parameter: $\tau = 1.0 \times 10^{-8}$

RESULTS: Three Square Cylinders $L = 0.16\lambda$

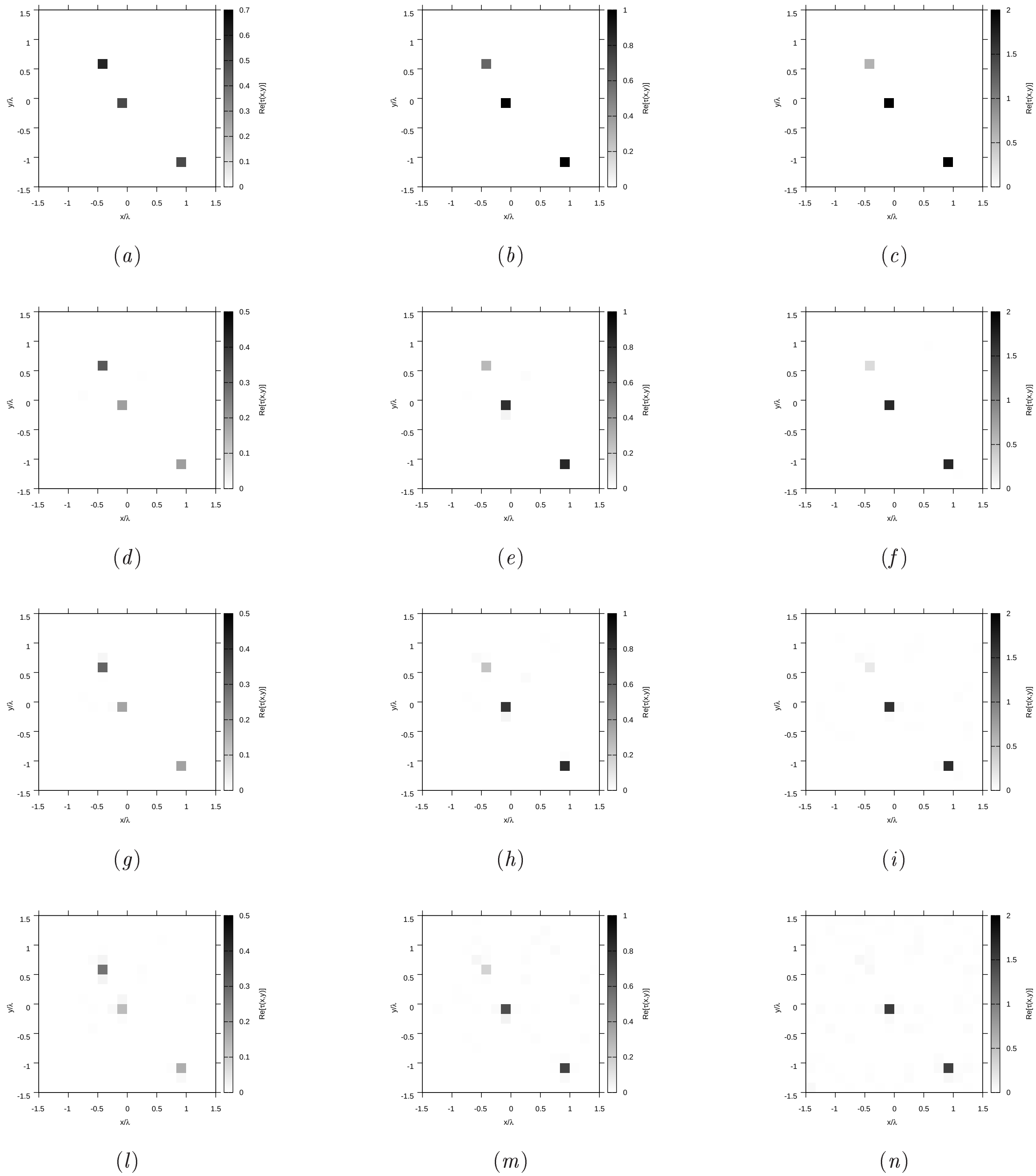

Figure 4. Actual object $(a)(b)(c)$ and BCS reconstructed object with $(d)(g)(l)$ $\varepsilon_r = 1.5$, $(e)(h)(m)$ $\varepsilon_r = 2.0$, and $(f)(i)(n)$ $\varepsilon_r = 3.0$, for $(d)(e)(f)$ Noiseless case, $(g)(h)(i)$ $SNR = 10$ [dB] and $(l)(m)(n)$ $SNR = 5$ [dB].

RESULTS: Three Square Cylinders $L = 0.16\lambda$ - Error Figures - Comparison Born/Rytov Approximation

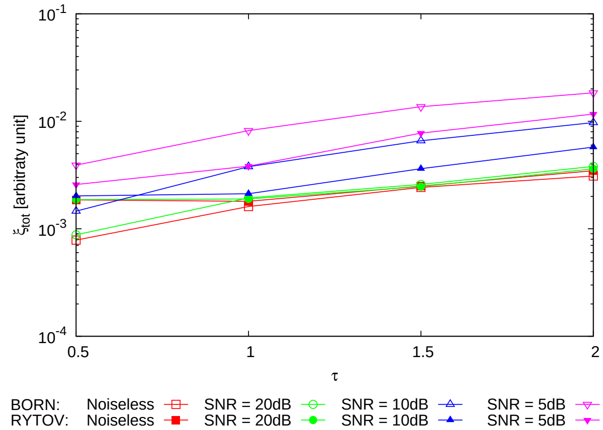

(a)

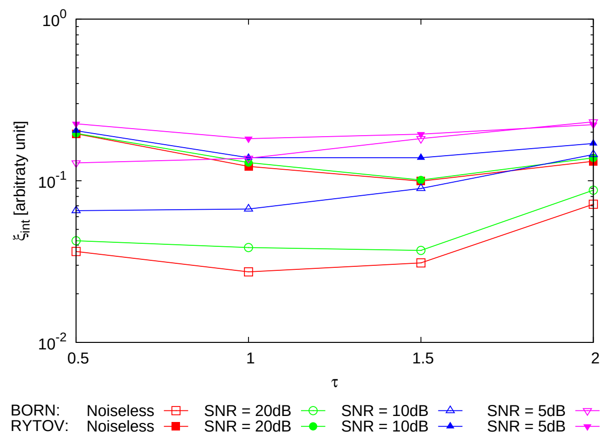

(b)

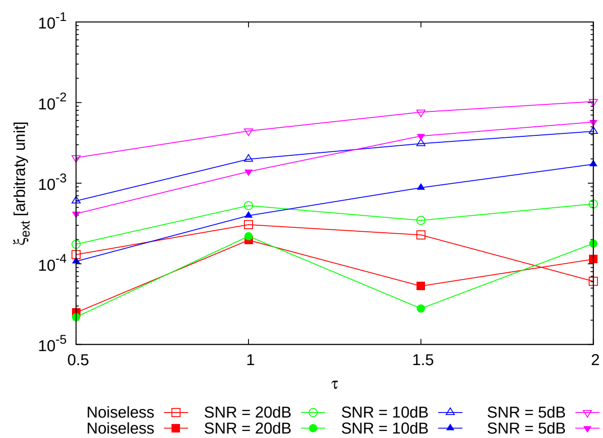

(c)

Figure 5. Behaviour of error figures as a function of ε_r, for different SNR values: (a) total error ξ_{tot}, (b) internal error ξ_{int}, (c) external error ξ_{ext}.

References

[1] L. Poli, G. Oliveri, and A. Massa, "Imaging sparse metallic cylinders through a Local Shape Function Bayesian Compressive Sensing approach," Journal of Optical Society of America A, vol. 30, no. 6, pp. 1261-1272, 2013.

[2] F. Viani, L. Poli, G. Oliveri, F. Robol, and A. Massa, "Sparse scatterers imaging through approximated multitask compressive sensing strategies," Microwave Opt. Technol. Lett., vol. 55, no. 7, pp. 1553-1558, Jul. 2013.

[3] L. Poli, G. Oliveri, P. Rocca, and A. Massa, "Bayesian compressive sensing approaches for the reconstruction of two-dimensional sparse scatterers under TE illumination," IEEE Trans. Geosci. Remote Sensing, vol. 51, no. 5, pp. 2920-2936, May. 2013.

[4] L. Poli, G. Oliveri, and A. Massa, "Microwave imaging within the first-order Born approximation by means of the contrast-field Bayesian compressive sensing," IEEE Trans. Antennas Propag., vol. 60, no. 6, pp. 2865-2879, Jun. 2012.

[5] G. Oliveri, P. Rocca, and A. Massa, "A bayesian compressive sampling-based inversion for imaging sparse scatterers," IEEE Trans. Geosci. Remote Sensing, vol. 49, no. 10, pp. 3993-4006, Oct. 2011.

[6] G. Oliveri, L. Poli, P. Rocca, and A. Massa, "Bayesian compressive optical imaging within the Rytov approximation," Optics Letters, vol. 37, no. 10, pp. 1760-1762, 2012.

[7] L. Poli, G. Oliveri, F. Viani, and A. Massa, "MT-BCS-based microwave imaging approach through minimum-norm current expansion," IEEE Trans. Antennas Propag., in press. doi:10.1109/TAP.2013.2265254

[8] G. Oliveri and A. Massa, "Bayesian compressive sampling for pattern synthesis with maximally sparse non-uniform linear arrays," IEEE Trans. Antennas Propag., vol. 59, no. 2, pp. 467-481, Feb. 2011.

[9] G. Oliveri, M. Carlin, and A. Massa, "Complex-weight sparse linear array synthesis by Bayesian Compressive Sampling," IEEE Trans. Antennas Propag., vol. 60, no. 5, pp. 2309-2326, May 2012.

[10] G. Oliveri, P. Rocca, and A. Massa, "Reliable Diagnosis of Large Linear Arrays - A Bayesian Compressive Sensing Approach," IEEE Trans. Antennas Propag., vol. 60, no. 10, pp. 4627-4636, Oct. 2012.

[11] F. Viani, G. Oliveri, and A. Massa, "Compressive sensing pattern matching techniques for synthesizing planar sparse arrays" IEEE Trans. Antennas Propag., in press. doi:10.1109/TAP.2013.2267195

[12] M. Carlin, P. Rocca, G. Oliveri, F. Viani, and A. Massa, "Directions-of-Arrival Estimation through Bayesian Compressive Sensing strategies," IEEE Trans. Antennas Propag., in press.

[13] M. Carlin, P. Rocca, "A Bayesian compressive sensing strategy for direction-of-arrival estimation," 6th European Conference on Antennas Propag. (EuCAP 2012), Prague, Czech Republic, pp. 1508-1509, 26-30 Mar. 2012.

[14] M. Carlin, P. Rocca, G. Oliveri, and A. Massa, "Bayesian compressive sensing as applied to directions-of-arrival estimation in planar arraysâ" Journal of Electrical and Computer Engineering, Special Issue on "Advances in Radar Technologiesâ" in press.

[15] M. Donelli, D. Franceschini, P. Rocca, and A. Massa, "Three-dimensional microwave imaging problems solved through an efficient multi-scaling particle swarm optimization," IEEE Trans. Geosci. Remote Sensing, vol. 47, no. 5, pp. 1467-1481, May 2009.

[16] M. Benedetti, G. Franceschini, R. Azaro, and A. Massa, "A numerical assessment of the reconstruction effectiveness of the integrated GA-based multicrack strategy," IEEE Antennas Wireless Propag. Lett., vol. 6, pp. 271-274, 2007.

[17] P. Rocca, M. Carlin, G. Oliveri, and A. Massa, "Interval analysis as applied to inverse scattering," IEEE International Symposium on Antennas Propag. (APS/URSI 2013), Chicago, Illinois, USA, Jul. 8-14, 2012.

[18] L. Manica, P. Rocca, M. Salucci, M. Carlin, and A. Massa, "Scattering data inversion through interval analysis under Rytov approximation," 7th European Conference on Antennas Propag. (EuCAP 2013), Gothenburg, Sweden, Apr. 8-12, 2013.

[19] P. Rocca, M. Carlin, and A. Massa, "Imaging weak scatterers by means of an innovative inverse scattering technique based on the interval analysis," 6th European Conference on Antennas Propag. (EuCAP 2012), Prague, Czech Republic, Mar. 26-30, 2012.

[20] S. C. Hagness, E. C. Fear, and A. Massa, "Guest Editorial: Special Cluster on Microwave Medical Imaging", IEEE Antennas Wireless Propag. Lett., vol. 11, pp. 1592-1597, 2012.

[21] G. Oliveri, Y. Zhong, X. Chen, and A. Massa, "Multi-resolution subspace-based optimization method for inverse scattering," Journal of Optical Society of America A, vol. 28, no. 10, pp. 2057-2069, Oct. 2011.

[22] A. Randazzo, G. Oliveri, A. Massa, and M. Pastorino, "Electromagnetic inversion with the multiscaling inexact-Newton method - Experimental validation," Microwave Opt. Technol. Lett., vol. 53, no. 12, pp. 2834-2838, Dec. 2011.

[23] G. Oliveri, L. Lizzi, M. Pastorino, and A. Massa, "A nested multi-scaling inexact-Newton iterative approach for microwave imaging," IEEE Trans. Antennas Propag., vol. 60, no. 2, pp. 971-983, Feb. 2012.

[24] G. Oliveri, A. Randazzo, M. Pastorino, and A. Massa, "Electromagnetic imaging within the contrast-source formulation by means of the multiscaling inexact Newton method," Journal of Optical Society of America A, vol. 29, no. 6, pp. 945-958, 2012.

[25] M. Benedetti, D. Lesselier, M. Lambert, and A. Massa, "Multiple shapes reconstruction by means of multi-region level sets," IEEE Trans. Geosci. Remote Sensing, vol. 48, no. 5, pp. 2330-2342, May 2010.

[26] M. Benedetti, D. Lesselier, M. Lambert, and A. Massa, "A multi-resolution technique based on shape optimization for the reconstruction of homogeneous dielectric objects," Inverse Problems, vol. 25, no. 1, pp. 1-26, Jan. 2009.